Journal of Computers Vol. 33 No. 2, April 2022, pp. 157-167
doi: 10.53106/199115992022043302014

The Pointer-type Instrument Recognition Method based on Yolov3

Shu-Qiang Guo*, Xian-Jin Li, Huan-Qiang Lin, Yue Lou, Jun-Cheng Li, Zhi-Heng Wang

School of Computer Science, Northeast Electric Power University, Jilin 132012, China
1339851898@qq.com

Received: 19 October 2021; Revised: 19 November 2021; Accepted: 24 November 2021

Abstract. In order to solve the problems of fuzzy image, different measuring range and recognition accuracy of pointer instrument in the process of power inspection, propose a pointer-type instrument recognition method based on Yolov3. Firstly, super-resolution technology is introduced to reconstruct the instrument image. Then, a combined Yolov3 and OCR- based dial feature extraction method is used to detect the dial in the instrument image, effectively extract the digital features in the region, and recognize the instrument by combining the digital features pointer-type angle. Next, to solve the instrument image's fuzzy problem, a super-resolution image reconstruction technology is designed to reconstruct the fuzzy instrument image and get a clear instrument image. Finally, a method based on a Yolov3 and OCR combination is proposed to detect the instrument image and recognize the digital features of the dial to target the insufficient use of dial features. Comparison of the effect of traditional machine learning algorithm and Canny edge detection in the pointer-type instrument image recognition shows that the accuracy and practicability of this method have been significantly improved in the recognition of pointer-type instruments in complex environment images.

Keywords: target detection, image reconstruction, Yolov3, OCR, pointer-type meter recognition

1 Introduction

There are a lot of ammeters, voltmeters, pressure gauges, oil level gauges, and other instruments in the power system. Because of the cost and historical reasons, most of these instruments are pointer-type instruments. pointer-type instrument has the advantages of simple structure and low cost and is not easy to produce electromagnetic interference. The pointer-type instruments are widely distributed. If manual inspection is used, it will consume a lot of human resources, and some harsh environments may endanger the personal safety of staff. Therefore, it is of great significance to study a fast, accurate and robust pointer instrument [1] identification method.

At present, there are many researches on the recognition of pointer-type instruments at home and abroad. Yao Yang and others used improved canny detection and Hough change instrument image recognition algorithm to improve Canny edge detection and improve the accuracy of edge detection, but the complexity is relatively high and the image quality requirements are high, so a double threshold selection method is needed. Firstly, the dial area is determined based on the region growing method, and then the improved central projection method is used to find the scale mark of the circular scale area. Finally, the Hough transform method is used to get the pointer-type feature through the pointer-type contour fitting, and the scale mark is used to get the range reading. Hough transform, image subtraction, and image thinning are used to get the center coordinates of the pointer-type, and the pixel data beyond the perimeter of the pointer-type in the image is removed. Combined with the Hough transform, the linear equation of the pointer-type is obtained. A recognition method of a pointer-type-type instrument based on binocular vision is proposed. The pointer-type features are detected by fast Hough transform and least square fitting technology. Based on the accurate three-dimensional space reconstruction of straight lines in the left and right display images, the pointer-type instrument readings are projected onto the target plane. The number recognition on the dashboard is carried out based on the combination of template matching and normalization [2], and the pointer-type features are obtained by radial projection and the Bresenham algorithm, which has high accuracy.

However, the current methods of pointer instrument recognition generally have some problems, such as poor image quality of pointer instrument, difficult to obtain the characteristics of pointer instrument, inaccurate reading of pointer instrument and so on. In the view of the shortcomings of traditional methods to deal with these problems, this paper proposes a method of pointer-type meter recognition based on deep learning [3]. The super-resolution technology is introduced to reconstruct the instrument panel image to improve the quality of the instrument

* Corresponding Author

image; the instrument target is detected with Yolov3, and then the detected instrument image is corrected and input to OCR for digital feature recognition [4]; the significance detection is used to detect the pointer-type feature, and the angle value is obtained by rotating line fitting method combined with the digital feature obtained in the second step Carry out instrument identification [5].

2 Image Characteristics and Recognition Model of Pointer-type Instrument

2.1 Characteristics of Pointer-type Instrument

1. The image of the pointer-type instrument is not clear enough. Because the environment of the pointer-type instrument is complex, or because of the distance, position, and other problems, the image of the pointer-type instrument has some interference. Moreover, most pointer-type instruments are not necessarily placed in a sheltered place, which may cause dust on the surface due to external environmental problems. In order to recognize the number of pointer-type meters correctly, it is necessary to obtain high quality and clear image and detect the meter, pointer-type, number, and scale line.

2. There are many kinds of pointer-type instruments. Because of the different manufacturers and uses of pointer-type instruments, the specifications of each pointer-type instrument may be different. Just from the user's point of view, there are an ammeter, voltmeter, thermometer, pressure gauge, and power meter. Even for the same kind of pointer-type instruments, there are problems such as different ranges.

3. The location of the cameras varies. In the process of acquiring the pointer-type instrument image, there are some reasons, such as road slope, illumination, camera angle, camera position, and so on, which lead to the deviation of the pointer-type instrument image.

In order to solve the above problems, this paper uses the super-resolution image reconstruction technology to reconstruct the possible fuzzy image to obtain the high-quality pointer-type instrument image and then uses the Yolov3 target detection technology to detect the pointer-type instrument area in the image. In addition, the measurement range and other information of the instrument are obtained by OCR digital recognition technology to analyze the pointer-type instrument image Calibration, and then calculate the pointer-type angle, and finally calculate the meter reading according to the range information and pointer-type angle.

2.2 Instrument Reading Recognition Model based on Yolov3

In view of the characteristics of pointer-type instrument images and the shortcomings of traditional pointer-type instrument recognition methods, this paper introduces the recognition technology of pointer-type instrument based on deep learning Yolov3 [6]. Firstly, the obtained pointer-type image is super-resolution reconstructed to obtain a high-quality image [7], and then the pointer-type instruments is recognized.

The idea of this paper is to first get the pointer-type instrument image super-resolution reconstruction processing, get a clearer high-quality image, and then input the obtained high-quality image into the pre-trained Yolov3 network to detect the pointer-type instrument, get the pointer-type instrument object, eliminate the background interference, and then input the pointer-type instrument image into the OCR network. Finally, the angle of the pointer-type is calculated and combined with the above digital features to identify the pointer-type instrument [8]. The processing flow chart is shown in Fig. 1:

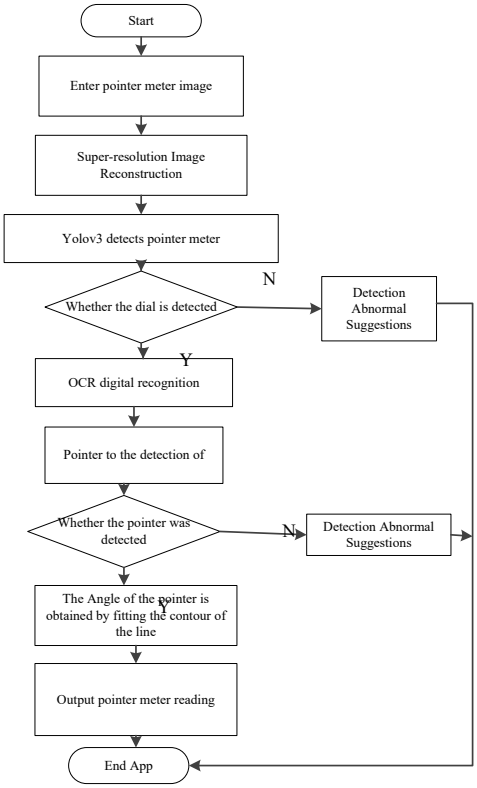

Fig. 1. Identification process of pointer-type instrument based on Yolov3

3 Pointer-type Instrument Detection

3.1 Target Detection Network Yolov3

At present, the deep learning network used in target detection [9] mainly includes SSD [10] and its extended network, R-CNN series, Yolo series, and so on. R-CNN [11] generates a series of sparse candidate frames by the heuristic method, and then classifies and regresses the candidate frames. The advantage of R-CNN is that it has high accuracy. Yolo series mainly conducts uniform dense sampling of images, adopts different scales and aspect ratios, and uses CNN [12] to extract features for classification and regression. The advantage is that it is relatively fast. In order to solve the problems of low accuracy and low speed in the process of pointer-type meter recognition, this paper puts forward a pointer-type meter recognition method based on Yolov3. In order to improve the operation speed, the convolution layer and BN layer of Yolov3 are combined, and the operation speed is improved to a certain extent while the accuracy remains unchanged, The IOU distance in the bounding box prediction is changed to GIOU distance, which solves the shortcomings of IOU and improves the accuracy.

The network structure of Yolov3 mainly includes two parts: Darknet-53 and the Yolo prediction branch. Darknet-53 was an improvement on the V2 Darknet-19, which is mainly composed of convolution layer, batch normalization layer, and thermocline layer. It performs better than Darknet-19 in classification accuracy and efficiency. The DBL structure in Fig. 2 is the basic structure of Yolov3, mainly including convolution layer, batch normalization layer, and activation function Leaky Relu. The darknet-53 structure is composed of residual units, which are mainly used for feature extraction of the input image. Because in the forward propagation process, after five convolution transformations, the feature image is reduced to 1 / 32 of the original, so the size of the input image should be a multiple of 32, here we take 416x416x3. In the process of predicting the bounding box, in order to select the appropriate size of the bounding box, a K-means clustering algorithm based on IOU distance is used to determine the size of the default box. There are nine default boxes selected by Yolov3. In the multi-scale prediction method adopted by Yolov3, convolution operation and feature map and local information fusion operation are used on the same scale Yolo to obtain the feature map Y1: (13x13), Y2: (26x26), Y3: (52x52) under three scales, and then target detection is carried out under three different scales.

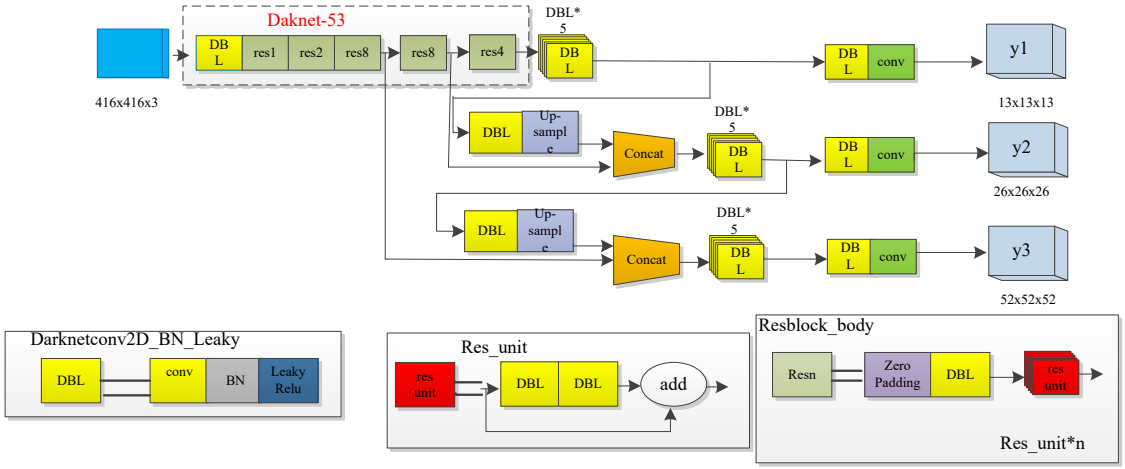

Fig. 2. Structure of Yolov3

In infrastructure DBL, the BN layer is used to adjust the parameters of SGD, such as learning rate, attenuation coefficient, drop-out ratio, parameter initialization, and so on. However, because a new BN layer is added, the structure of the whole model becomes more complex, and the computational cost increases. In the process of bounding box prediction, there may be more than one prediction box for the same target. We need to select the prediction box with the highest score to keep it. For calculating the prediction box and the target box, we need to use the IOU to judge the positive and negative samples of the target box. Only if the prediction box and the target box are IOU>0.5 and the category are the same it means that the prediction is correct. According to the definition, IOU distance exists when the prediction frame and the target frame do not intersect, IOU = 0, which can not reflect the coincidence degree of the two, so it can not be used for learning and training.

In this paper, the convolution layer and BN layer of DBL structure are combined to reduce the network complexity and improve the operation speed while ensuring the detection results; the IOU distance formula is changed to GIOU distance to solve the problem that the similarity between the prediction frame and the target frame can not be obtained when there is no intersection between them without reducing the accuracy.

3.2 Improvement of Yolov3

3.2.1 Combining Convolution Layer and BN Layer

In the DBL structure, it can be seen that the BN layer is behind the convolution layer and before the activation function. The function of the BN layer is to normalize the data, effectively solve the problems of gradient disappearance and gradient explosion, accelerate the network convergence and control the occurrence of the over-fitting phenomenon. Although the BN layer has the above positive role, because of the addition of a layer, the operation speed has a certain impact and takes up more memory and video memory. Therefore, we can combine the BN layer into the convolution layer to improve the operation speed of the model. (Fig. 3)

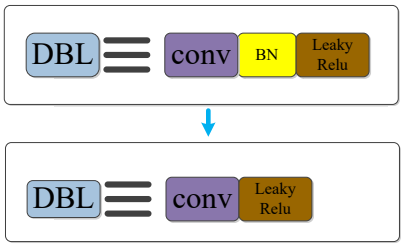

Fig. 3. DBL model

$$out[j]=\sum_{i=0}^{n}(x_i * w_i) \tag{1}$$

$$bn[j]=gamma*(out[j]-mean)/sqrt(variance)+beta \tag{2}$$

The convolution layer obtains the information in the picture by using the out function to convert the matrix of each channel from left to right and from top to bottom, and then inputs the obtained information into the BN layer to accelerate the network convergence and control the over fitting. In this paper, BN layer is combined into convolution layer, and the coefficients are adjusted directly after feature extraction in convolution layer. Finally, the new offset and weight are saved in the weight file.

$$bn=\sum_{i=0}^{n}(x_i*grmma*w_i/sqrt(variance))-grmma*mean/sqrt(variance)+bet \tag{3}$$

$$b_{new}=grmma*(b-mean)/sqrt(variance)+bet \tag{4}$$

$$w_{new}=grmma*w/sqrt(variance) \tag{5}$$

The new bias and weight obtained by using the above formula are the same as those obtained by original convolution and batch normalization in the BN layer, and the speed has been improved to a certain extent. Therefore, we can delete the BN layer, and only need to adjust the bias and weight of the convolution layer to b_{new} and w_{new}, and then write it to the new weight file.

3.2.2 Using GIOU Distance in Boundary Box Regression

There is no big change in the prediction of the initial size of the bounding box in Yolov3, which uses the K-means clustering algorithm in V2 to calculate. This kind of prior knowledge is of great help to the initialization of the bounding box. In K-means clustering, V2 uses the anchor mechanism of fast R-CNN instead of the original default box size and uses the measurement loss calculated by IOU instead of regression loss.

As a measure of distance, the IOU function includes nonnegativity, uncertainty symmetry, and trigonometric inequality. In addition, IOU has scale invariance, which means that the similarity of any two boxes A and B is independent of their spatial scale. But the IOU distance also has some disadvantages, that is, it is only applicable to the intersection of two objects, if two objects do not intersect, the IOU distance is not applicable. As shown in Fig. 4 below:

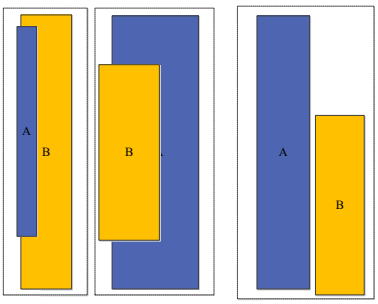

Fig. 4. Schematic diagram of IOU distance

$$IOU=|A\cap B|/|A\cup B| \tag{6}$$

A is the prediction box and B is the real box. If two objects do not overlap, the value of IOU will be zero, which cannot reflect the distance between the two shapes. If the two objects do not overlap, then the IOU is used as the loss value is zero, and the performance cannot be optimized. If $|A\cap B|=0$, then $IOU(A,B)=0$. Therefore, in order to achieve the same function as the IOU, that is, to encode the shape attribute of the comparison object as

the region attribute, at the same time to keep the original scale of the IOU without deformation and to achieve the strong correlation of the IOU when the bounding box overlaps the object. So here we use GIOU instead of IOU (Fig. 5):

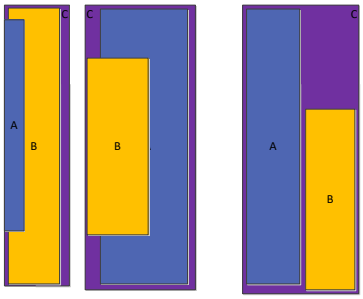

Fig. 5. Schematic diagram of GIOU distance

$$GIOU=|A\cap B|/|A\cup B|-|C-(A\cup B)|/|C| \quad \textbf{(7)}$$

A is the prediction box, B is the real box, and C is the smallest box that can cover A and B. For any box A and B, first, find the smallest box C that can completely cover them, and then calculate the IOU value of A and B minus C minus the proportion of the intersection of A and B in C to get GIOU.

$$d(box,centroid)=1-IOU(box,centroid) \quad \textbf{(8)}$$

Centroid is the bounding box selected as the center, the box is the other bounding boxes, and d is the distance between the other bounding boxes and the center bounding box. The larger the IOU value is, the closer the distance is.

Under certain conditions, the value of IOU and the value of GIOU overlap, and the range of GIOU is - 1 to 1, while the range of IOU is 0 to 1. For a more intuitive comparison of their value ranges, the Fig. 6 shows the data overlap comparison between IOU and GIOU:

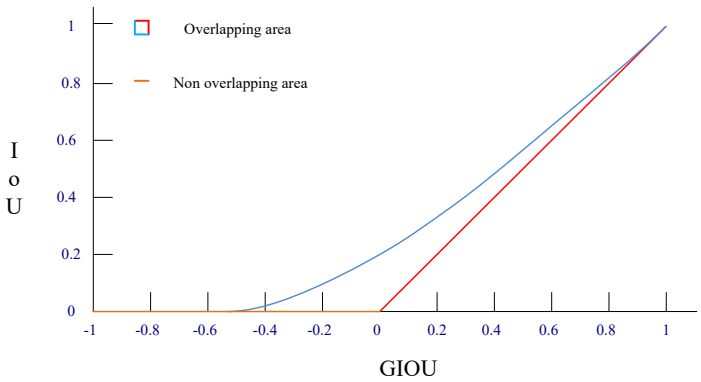

Fig. 6. GIOU and IOU chart

3.3 Application of Improved Yolov3 in Instrument Detection

In order to improve the detection accuracy [13] of the pointer-type instrument, we first use Yolov3 to detect the area of the pointer-type instrument in the image of the pointer-type instrument and then recognize the number of the pointer-type instrument area. The open-source tool Labellmg is used to make the data set of Yolov3. The pointer-type instrument is selected in the pointer-type instrument image, and the corresponding label is input. After the completion of the training set, the images are input into the network for training. In order to improve the

accuracy of pointer-type meter detection and improve the training speed, Darknet-53 is pre-trained in this paper.

Before the pointer-type instrument segmentation task, we need to test the target detection performance of Yolov3 separately. Fig. 7 shows the test results of detecting dial area in a single pointer-type meter by Yolov3, and Fig. 8 shows the test results of recognizing multiple pointer-type dial areas in the image by Yolov3, Fig. 9 shows the recognition results of the complete pointer instrument in the yolov3 recognition image, as shown in the following figure:

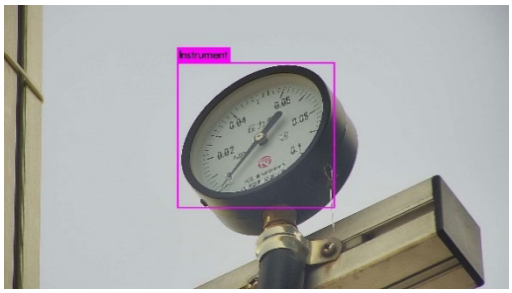

Fig. 7. Single-dial test results

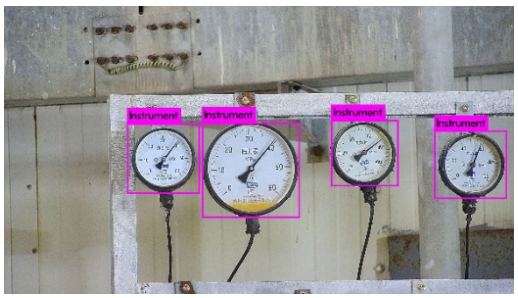

Fig. 8. Multiple dial test results

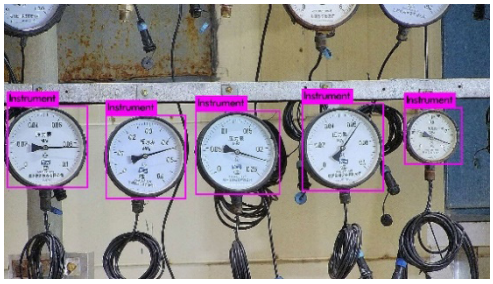

Fig. 9. Integrity dial detection

From the test results obtained, the improved Yolov3 can detect the pointer-type instrument area in the image with high confidence under different distance and illumination conditions, and recognize the types of pointer-type instrument targets in the area, and the speed has been improved to a certain extent, which indicates that the Yolov3network training result is ideal. Fig. 8 shows that in a pointer-type instrument image with multiple dials and incomplete dials in a complex environment, only available dials can be detected without being misled by incomplete dials.

4 Pointer-type Instrument Identification

4.1 OCR Digital Recognition

The process of digital recognition is divided into the following parts: first, the pre-processing operation of the processed pointer-type image is processed, and the image of the instrument is grayscale to reduce the amount of information and reduce the amount of computation. Because Baidu Intelligent Cloud already has a more accurate OCR digital recognition technology, here we will input the image to be recognized by the gray preprocessed image to Baidu OCR digital recognition; then through the completion of API request creation and parameter setting, processing response or exception, finally input text information to realize OCR digital recognition.

4.2 Pointer-type Detection and Reading Recognition

Saliency detection is widely used in image segmentation, edge detection, image index, and object detection. Saliency detection is to calculate the importance of each information in the image through computer simulation of human visual attention mechanism and get the gray image. According to the saliency value of each pixel in the gray value, we can get the saliency image, and then get the saliency region we need to achieve saliency detection. The subtables in Fig. 10(a) and Fig. 10(b) show the pointer-type dashboard images in the original picture and in the case of saliency detection:

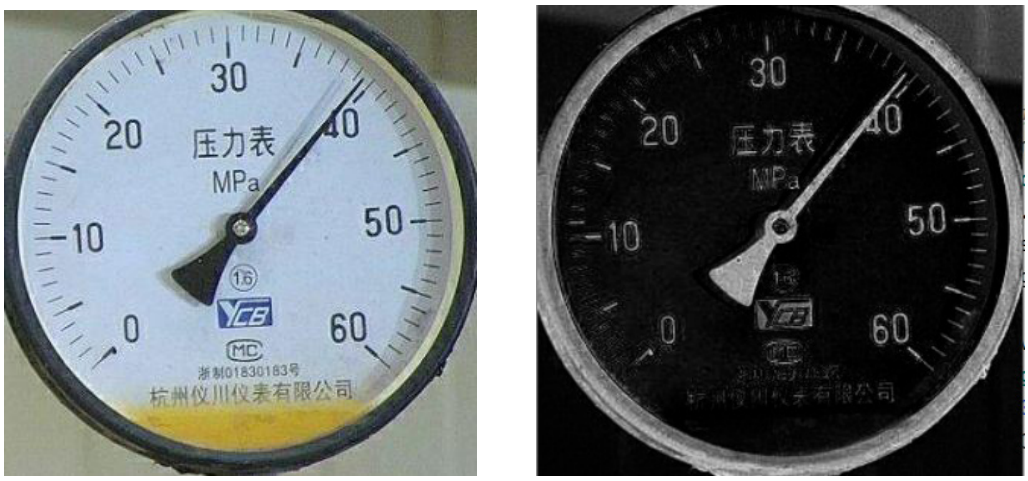

(a) Dial area (b) Significance detection area

Fig. 10. Effect picture of significance detection of the instrument panel

Saliency detection in this paper is to get the saliency value by comparing the whole image with each sub-region of the image. The high-frequency part represents the texture details of the image, and the low-frequency part represents the edge and contour information of the image. In the frequency domain, the Gauss difference formula is used to filter and extract the significant region. The Gauss difference formula is:

$$Dox(x,y)=G(x,y,\sigma 1)- G(x,y,\boldsymbol{\sigma} 2) \quad \textbf{(9)}$$

Through the above pointer-type line detection processing, we can get the point coordinates (x, y) of the pointer-type line and the vertex coordinates (p, q) of the pointer-type line after pointer-type rotation. by OCR digital recognition, we can get the position of the starting and ending scale line, so we can connect the midpoint position of the scale line and the line where the center of the pointer-type instrument is to become the endpoint of the long scale line. The line connecting the vertex of the pointer-type and the circle point of the pointer-type instrument is the pointer-type rotation line. According to the definition of the line slope, we can calculate the slope of the line, (x_i, y_i) , (x_j, y_j) are the two coordinates on the straight line [14], which represent the coordinates of the pointer-type circle point and the center point of the scale line. The inclination angle of the straight line can be calculated. The calculation formula is as follows:

$$\beta=arctan(y_i-y_j)/(x_i-x_j) \quad \textbf{(10)}$$

x. y is the coordinate on the straight line according to the coordinates of two points on the straight line. Calculate the inclination angle of the starting scale line and the pointer-type line, and then calculate the inclination angle of the pointer-type line based on the upper scale line. Then according to the angle parameters of the upper and lower scale lines of the pointer-type instrument range, combined with the inclination angle of the starting scale line and the pointer-type rotation line, the indicator of the pointer-type instrument can be directly calculated, so as to realize the recognition of the pointer-type instrument [15].

5 Analysis of Test Results

5.1 Test Situation and Evaluation Index

The super-resolution image reconstruction has been implemented in the testing of the pointer-type instrument recognition method based on Yolov3 and OCR, and it is not described too much. This paper focuses on the test of the automatic recognition effect of instrument reading in Yolov3 target detection and OCR digital recognition technology. In order to select more than 1000 transformer substation instruments as the experimental data set of pointer-type instrument identification. The resolution of each image is 640x480, including pressure gauge, ammeter, pointer-type instrument at a high place, and pointer-type instrument at a low position. For the experimental

data set, 1000 pointer-type instrument images are selected as training sets and 100 images as test sets according to the ratio of 10:1. After 1000 pointer-type instrument images are trained according to the method described in this paper, 50 test sets are selected to detect whether the target detection can be effectively performed in a multi-objective environment, single target environment, and complex environment. After testing, the accuracy of the pointer-type instrument identification model based on Yolov3 can reach 98% after 500 rounds of testing training. It can eliminate the interference accurately and identify the pointer-type instrument. The test platform environment is: Ubuntu 16.04, NVIDIA RTX2080TI, Intel Xeon(R) Silver 4116 @2.1GHz × 48.

5.2 Analysis of Instrument Test Results

The test results of the pointer-type instrument test task are shown in Table 1.

Table 1. Analysis of test results of pointer-type instrument

Model	Average accuracy (%)	Detection rate(s)
Yolov3	85.01	35
yolov2	81.09	66
Faster R-CNN	82.24	8
SSD	46.5	20

Through the test results of several models, it can be found that the model based on Yolov3 has both the average accuracy and the detection rate. The miss detection rate of this model is low, and the target can be detected in most cases, but there may be miss detection in the case of multiple occlusion or long distance. In this case, the pointer-type instrument will be further image acquisition, and then the recognition of the pointer-type instrument will be carried out to improve the accuracy of Yolov3 target detection.

5.3 Analysis of Pointer-type Test Results

The following Fig. 11 compares the methods of significance detection, Hoff linear transformation, edge detection, and other methods to detect the existence of pointer-type. From Fig. 11(a), it can be seen that although the pointer-type line detected by Hoff linear transformation is clear, there are some red light point straight lines; Fig. 11(b) is the significant linear detection method adopted in this model, which can detect the pointer-type clearly The pointer-type memory detected by Fig. 11(c) edge detection method is a pointer-type line composed of multiple segments, which cannot show the pointer-type line completely, which has some virtualization; the linear detected by Fig. 11(d) LSD linear detection method has the same effect as the edge detection line, basically, it is a pointer-type line composed of some segments, but the small size of LSD linear detection algorithm The length of the line segment is longer than the edge detection, and the radian and effect are not good for edge detection. Comparing with the above several straight-line methods, it can be found that the significant linear detection method used in this paper can eliminate interference and get a clear identification of the pointer-type line.

(a) Hoff linear test

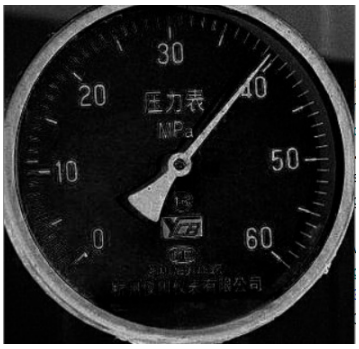

(b) Significance test

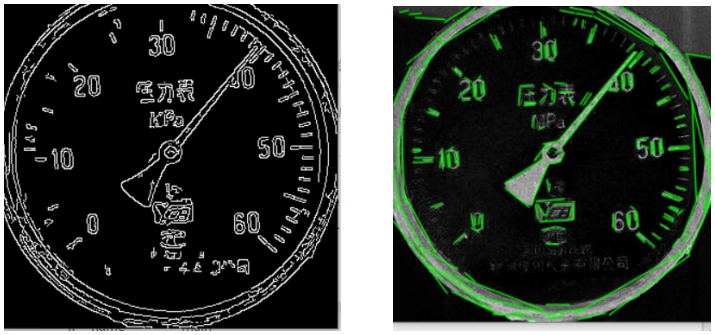

(c) Edge detection (d) LSDLSD line detection

Fig. 11. Comparison of the pointer-type detection

5.4 Analysis of Instrument Reading Recognition Results

The analysis of reading recognition results of the pointer-type instrument is shown in Table 2.

Table 2. Analysis of instrument reading results

Model	Error detection rate (%)	Recognition accuracy rate (%)	Time consuming (s)
Yolov3	0	91.12	0.031
Faster-R_CNN+U-Net	0	87.3	0.125
HOG+SVM	1.35	85.34	3.98

Through Table 2, it can be found that the pointer-type instrument recognition method based on Yolov3 is significantly higher than other models in detection rate, recognition accuracy, and time-consuming. The recognition method of the pointer-type instrument based on Yolov3 also has the following situations in the actual process. For the pointer-type instrument image in Fig. 12(a), it is the easiest to identify, because the pointer-type instrument image is clear, and the pointer-type instrument can be detected, and the digital feature, range, and scale mark feature can be easily identified, so it can have a better recognition effect; as can be seen in Fig. 12(b), in this pointer-type instrument image, we can detect the pointer-type instrument, However, because the pointer-type instrument has been used for a long time, under the influence of the sun exposure and outdoor dust, the plastic surface of the outer frame is blurred, and there is no way to identify the internal scale line and digital features. As can be seen from Fig. 12(c), a complete pointer-type meter in the image of pointer-type meter can be detected to carry out the following process of pointer-type meter identification. However, there are still three partially occluded meters in the upper frame of the picture, so it is impossible to accurately read the pointer-type meter degree.

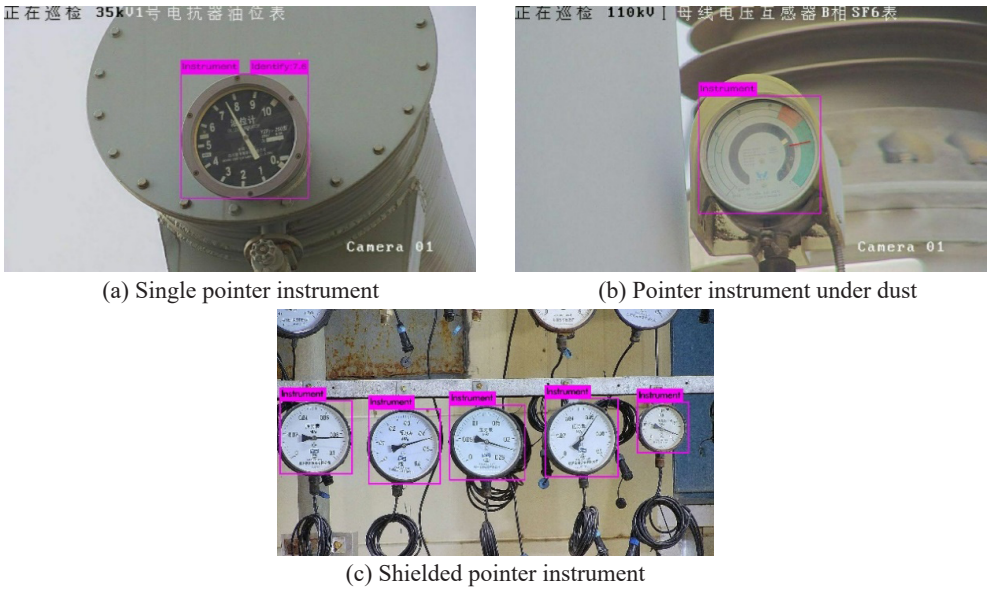

(a) Single pointer instrument (b) Pointer instrument under dust

(c) Shielded pointer instrument

Fig. 12. Analysis chart of instrument reading recognition results

6 Conclusion

In order to improve the recognition effect of the pointer-type instruments, it is necessary to have a high-quality pointer-type instrument image. The traditional method is to improve the pointer-type instrument image by image preprocessing. In this paper, we propose a super-resolution image reconstruction algorithm based on deep learning to improve the clarity of the pointer-type instrument image. It provides a high-quality image for pointer-type meter recognition.

A feature detection method of the pointer-type instrument based on the combination of Yolv3 and OCR is proposed, which abandons the traditional edge detection algorithm and uses the deep learning Yolo series target detection method to get the target object of the pointer-type instrument. In order to improve the accuracy of small target detection of pointer-type instruments, the Yolv3 target detection method is adopted. In order to solve the problem of a different range of different instrument panels, the OCR digital recognition technology is adopted. By extracting the dial information on the pointer-type instrument, the indicator of the pointer-type instrument is output according to the range and angle value of different pointer-type instruments.

The method in this paper is also applicable to the detection and identification of other digital equipment components, and plays an important role in the real-time dynamic monitoring of technical data changes, so as to further improve the intelligent level of digital equipment identification.

References

[1] H. Zhang, B. Su, H. Meng, Development and implementation of a robotic inspection system for power substations, The Industrial Robot 44(3)(2017) 333-342.
[2] J. Chi, L. Liu, J. Liu, Z. Jiang, G. Zhang, Machine Vision Based Automatic Detection Method of Indicating Values of a Pointer Gauge, Mathematical Problems in Engineering 2015(2015) 283629.
[3] J. Schmidhuber, Deep learning in neural networks: An overview, Neural Networks 61(2015) 85-117.
[4] X. Ye, D. Xie, S. Tao, Automatic Value Identification of Pointer-Type Pressure Gauge Based on Machine Vision, Journal of Computers 8(5)(2013) 1309-1314.
[5] B. Yang, G. Lin, W. Zhang, Auto-recognition Method for Pointer-type Meter Based on Binocular Vision, Journal of Computers 9(4)(2014) 787-793.
[6] P.A. Belan, S.A. Araujo, A.F.H. Librantz, Segmentation-free approaches of computer vision for automatic calibration of digital and analog instruments, Measurement 46(1)(2013) 177-184.
[7] P. Li, Q. Wu, Y. Xiao, Y. Zhang, An efficient algorithm for recognition of pointer scale value on dashboard, in: Proc. 2017 10th International Congress on Image and Signal Processing, BioMedical Engineering and Informatics (CISP-BMEI). IEEE, 2017.
[8] Z. Ding, B. Feng, W. Mo, Automobile Dashboard Object Recognition for Interested Vehicle in ITS, in: Proc. 2019 IEEE 4th Advanced Information Technology, Electronic and Automation Control Conference (IAEAC), 2019.
[9] Z. Rui, Z. Tao, Y. Li, The design of a portable inspection and reading system for instrument panel, Machinery, 2016.
[10]A. Ivaschenko, A. Krivosheev, D. Sveshnikov, N. Svechkov, T. Feschenko, Y, Tyshkovskaya, A. Chuvakov, Intelligent Recognition in Automated Meters Surveying, in: Proc. 2020 27th Conference of Open Innovations Association (FRUCT). IEEE, 2020.
[11]Y. Peng, Z. Chen, Application of Deep Residual Neural Network to Water Meter Reading Recognition, in: Proc. 2020 IEEE International Conference on Artificial Intelligence and Computer Applications (ICAICA). IEEE, 2020.
[12]X. Zhang, X. Dang, Q. Lv, S. Liu, A Pointer Meter Recognition Algorithm Based on Deep Learning, in: Proc. 2020 3rd International Conference on Advanced Electronic Materials, Computers and Software Engineering (AEMCSE). IEEE, 2020.
[13]G. Liu, J. Gu, J. Zhao, F. Wen, G. Liang, Super Resolution Perception for Smart Meter Data, Information Sciences 526(2020) 263-273.
[14]J. Liu, H. Wu, Z. Chen, Automatic Identification Method of Pointer Meter under Complex Environment, in: Proc. of the 2020 12th International Conference on Machine Learning and Computing, 2020.
[15]J. Zhu, W. Huang, W. Chen, X. Zhang, An Ellipse Fitting with PSO for Automatic Reading Recognition of Pointer Instruments, in: Proc. International Conference on Intelligent Autonomous Systems, 2019.